



# Influence of the surface processes on the hydrogen permeation through ferritic steel and amorphous $\text{Fe}_{40}\text{Ni}_{40}\text{Mo}_4\text{B}_{16}$ alloy specimens

J.S. Georgiev<sup>\*</sup>, L.A. Anestiev

*Institute for Metal Science, Bulgarian Academy of Sciences, 67 Shipchenski Prohod Str., 1574 Sofia, Bulgaria*

Received 25 March 1997; accepted 1 July 1997

## Abstract

A method for the determination of the gas diffusion coefficient  $D$  through thin membranes has been developed taking into account the membrane surface kinetic processes. The hydrogen permeation through STE890 steel and the amorphous alloy  $\text{Fe}_{40}\text{Ni}_{40}\text{Mo}_4\text{B}_{16}$  has been investigated in a wide temperature range with the aid of a method developed by the authors. It is shown that the theoretical and experimental approach developed for the determination of hydrogen diffusivity and permeation provides the possibility to gain reasonable results and can be successfully used for further studies. A criterion was set out to determine when the surface kinetic processes should be taken into account. The permeation and diffusion coefficients obtained with the aid of the present method, show a good correlation with those obtained by other authors with other methods. © 1997 Elsevier Science B.V.

## 1. Introduction

Hydrogen permeation in metals and alloys is a complicated phenomenon including several successive stages: adsorption, dissociation, dissolution, diffusion, recombination and desorption. Until now it is a general opinion that the surface processes play an insignificant role in the gas permeation through metals and alloys since it is considered that they are much faster than the diffusion itself [1–16]. This is probably true in the case of relatively thick specimens [13]. Unfortunately in some cases the specimens investigated cannot be made thick enough to eliminate the influence of the surface reactions on the processes of gas permeation. For example, this problem is encountered in the study of gas permeation through amorphous metallic alloys, where the preparation of specimens thicker than 50  $\mu\text{m}$  is physically impossible, or when the experimental set-ups do not allow investigations of thicker specimens. It should be also noted that the investigation of gas permeation on relatively thick specimens requires longer experimental periods.

The classical approach for the determination of the gas diffusion coefficient  $D$  in metals and alloys is based on the solution of the second order differential equation, known as second Fick's equation. For the permeated gas quantity  $Q(t)$  through a thin membrane of thickness  $l$ , the latter yields the well known dependences [1–3]

$$Q(t) = J(\infty)S \left\{ t - \frac{l^2}{6D} \right\} = J(\infty)S \{ t - \tau_D \}$$

$$\text{and } J(\tau_D) = 0.6299J(\infty).$$

In the above equations the quantities  $l$ ,  $S$  and  $\tau_D$ , are measured experimentally and they can be conveniently used for determination of the diffusion coefficient  $D$  [1–6]. Here  $J(\infty)$  is the stationary gas flux at  $t \rightarrow \infty$ ,  $\tau_D = l^2/6D$  is the delay time due to the diffusion process,  $S$  is the surface area of the specimen and  $t$  is the time. Note that the delay times  $\tau_D$ , determined with each of both the equations quoted above should be equal. Very frequently, the analysis of the experimental permeation data, using the above cited equations, shows a discrepancy between both delay times. For example, this is the case shown in Fig. 1 where the delay times determined with both equations differ almost by a factor of two from each other. The observed discrepancy between the values of  $\tau_D$  is due to

<sup>\*</sup> Corresponding author.

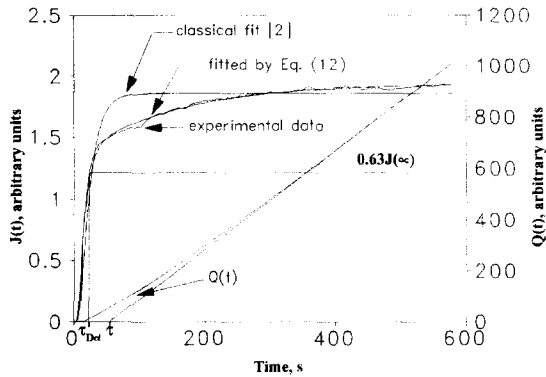


Fig. 1. A typical experimental curve obtained by the permeation experiments on STE890 steel specimen covered with thin layer from Pd ( $T = 673$  K,  $l = 0.001$  m,  $S = 3.14 \times 10^{-4}$  m<sup>2</sup> and  $P_{H_2} = 1.5$  kPa). The best fitted lines obtained by a non-linear regression of the experimental data, using Eq. (10) and the classical solution of the Fick equation, together with the permeated gas quantity  $Q(t)$ , are shown as a function of the time. The intercept of the  $Q(t)$ -asymptote with the time axis  $\tau$ , shows the total delay time of the permeation process. The value  $\tau_{Del} - J(\tau_{Del}) = 0.6299 J(\infty)$  [2] shows the expected delay time using the results based on the classical Fick's theory.

the existence of kinetic processes, taking place simultaneously with diffusion which explains the considerable increase of the delay time. The analysis of the experimental data of gas permeation through thin membranes obtained by us, using different theories dealing with this phenomena [1–4,7,10,12,13,16–24,31], showed that the most probable explanation of the increase of the delay time is the exis-

tence of surface reactions on the inlet surface of the studied specimens.

The question about the influence of the surface reactions on the hydrogen diffusivity is still unclear and as far as we know, there does not exist a detailed and self-consistent theoretical description which takes into account the processes in question [10,12,13,17–24,31]. Therefore, the theoretical and experimental study of this phenomena will lead to its elucidation and will allow a proper treatment of the experimental gas permeation data.

The aim of the present study is to develop suitable theoretical and experimental techniques in order to gain quantitative information on the hydrogen permeation mechanism in alloys also in the cases, where rates of the surface processes are comparable with those of the gas permeation processes.

## 2. Experimental approach

The principle scheme of our computer controlled experimental equipment developed on the basis of a MI 1201 mass-spectrometer is described in detail in our previous studies [4,6]. The diffusion cell consists of inlet and outlet chambers separated by the studied specimen. The specimen with exactly known surface area ( $3.14 \times 10^{-4}$  m<sup>2</sup>) and thickness (1 mm) is mounted between the cell flanges. A high vacuum of  $10^{-6}$ – $10^{-7}$  Pa is reached in both cell chambers with the aid of the high vacuum pumping sets of the mass-spectrometer MI-1201 B and a SNI-3 (system for introduction of isotopes) apparatus. The scheme of SNI-3

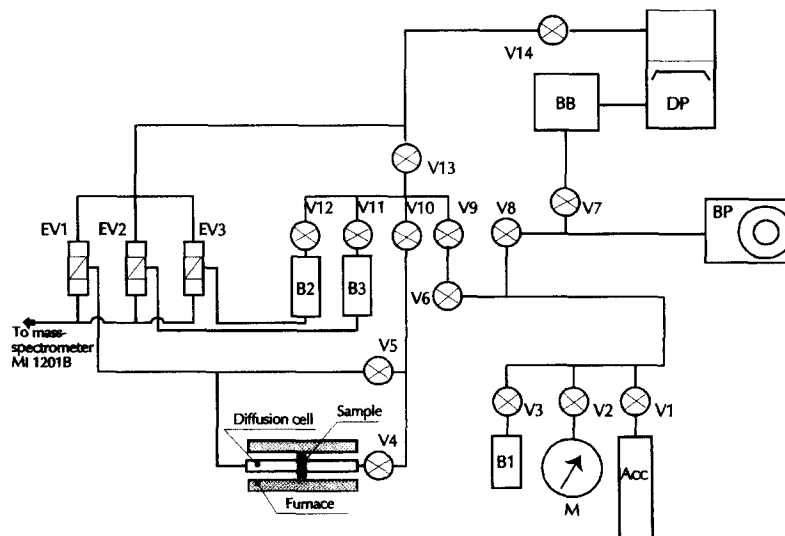


Fig. 2. Principle scheme of SNI-3 (system for introduction of isotopes) and the diffusion cell. V1 to V14 – high vacuum valves; EV1 to EV3 – electromagnetic valves; B1 – buffer volume; B2 and B3 – calibration volumes; M – pressure gauge; Acc – source for pure hydrogen; BP – backing pump; DP – diffusion pump; BBB – backing volume.

and the diffusion cell in question is shown in Fig. 2. After pumping, the diffusion cell heating unit is switched on in order to clean carefully the surface of the specimen. This cleaning is carried out in order to remove the adsorbed gases (O<sub>2</sub>, CO<sub>2</sub>, H<sub>2</sub>O, etc.), since these surface gas contamination hinder, and in some cases can even cause a strong reduction of hydrogen permeation into the specimen. After degassing of the inlet working surface of the specimen (membrane) and reaching the desired working temperature, a high purity (99.9999%) hydrogen from a solid state hydrogen accumulator is introduced into the inlet chamber. The filling time  $t_{\text{fil}}$  for all pressures studied ( $p = 5$  to  $7 \times 10^4$  Pa) was  $t_{\text{fil}} < 0.5$  s. The change of the gas flux passing through the membrane  $J$  is monitored as a function of time with the aid of the mass-spectrometer. After reaching a stationary state gas flux  $J(\infty)$ , the hydrogen is pumped out from the inlet chamber. This procedure is carried out for all pressures studied.

### 3. Theoretical approach

In order to determine the hydrogen diffusion coefficient  $D$ , taking into account the presence of surface reactions on the inlet surface of the studied specimen, it is necessary to solve the equations describing simultaneously the surface processes with the 2nd Fick equation, which accounts for the diffusion process through the membrane. This is not an easy task from the mathematical point of view [25,32], since both processes closely interact with each other. It is shown below that the kinetic processes which take place on the surface of the specimen determine the boundary conditions of the diffusion equation.

#### 3.1. Formulation of the problem

As it was mentioned above the gas permeation through a membrane includes the following successive processes: adsorption of the gas molecules on the inlet surface of the membrane, dissociation of the gas molecules to atoms and dissolution of the gas atoms, i.e., transition of the adsorbed gas atoms from the surface into the volume of the specimen and diffusion through the membrane [17–24,26,27].

These processes can be described mathematically by the following system of kinetic equations:

$$\frac{d\theta_m}{dt} = k_{\text{ads}} p (1 - \theta_a - \theta_m) - k_{\text{des}} \theta_m - k_{\text{diss}} \theta_m + k_{\text{rec}} \theta_a^2, \quad (1)$$

$$\frac{d\theta_a}{dt} = k_{\text{diss}} C (1 - \theta_a - \theta_m) - k_{\text{sol}} + k_{\text{diss}} \theta_m - k_{\text{rec}} \theta_a^2, \quad (2)$$

$$\frac{dC}{dt} = -k_{\text{diss}} C (1 - \theta_a - \theta_m) + k_{\text{sol}} \theta_a - \gamma J_D. \quad (3)$$

Here,  $\theta_m$  and  $\theta_a$  denote the fractions of the available adsorption sites occupied by gas molecules and gas atoms, respectively,  $p$  is the gas pressure,  $C$  is the dissolved gas concentration in the membrane surface in molar fractions,  $J_D$  accounts for the change of  $C$  with time due to diffusion,  $k_{\text{ads}}$  and  $k_{\text{des}}$  are the adsorption and the desorption kinetic coefficients,  $k_{\text{diss}}$  and  $k_{\text{rec}}$  are the kinetic coefficients of dissociation of the gas molecules and of recombination of the gas atoms,  $k_{\text{sol}}$  and  $k_{\text{dsol}}$  are the kinetic coefficients of solution and dissolution, respectively and  $\gamma$  is a coefficient which equates the dimension between  $C$ ,  $\theta_a$  and  $J_D$ . Here it is assumed that the gas molecules are di-atomic. In the above system of equations, Eq. (1) describes the balance of the adsorption sites on the surface occupied by gas molecules. The first two members of the right-hand side of this equation account for the influence of the adsorption and the desorption processes on the  $\theta_m$  balance. The second two members account for the influence of the dissociation and recombination processes respectively, i.e., in our particular case the reaction  $\text{H}_2 \leftrightarrow 2\text{H}$ . Eq. (2) describes the balance of the adsorption sites occupied by gas atoms. The first two members of the right-hand side of Eq. (2) account for the influence of the processes of solution of the adsorbed gas atoms and dissolution of the solved gas atoms on the  $\theta_a$  balance. The second two members coincide with these in Eq. (1), but are multiplied by a negative sign, since the dissociation process leads to an increase of the  $\theta_a$  sites, as the recombination processes lead to their decrease. The balance of the gas concentration  $C$  dissolved in the membrane, is given by Eq. (3).

The diffusion process through the membrane is described by the classical Fick equation [25]. Since in our case the physical conditions are equal for the whole surface of the studied specimen, a discussion of the one-dimensional problem is only necessary:

$$\frac{\partial C}{\partial t} = D \frac{\partial^2 C}{\partial x^2} \quad (4)$$

with initial and boundary conditions:

$$\begin{aligned} t = 0: C &= 0 \\ x = 0: C &= C(0, t) \\ x = l: C &= 0 \end{aligned}$$

Here the origin of the co-ordinate system is taken on the inlet surface of the studied specimen (membrane). Note that  $C(0, t)$  is an unknown time dependent function, which should be determined from the solution of Eqs. (1)–(3). The system of Eqs. (1)–(4) formulated in this way describes explicitly the diffusion through a thin membrane taking into account all kinetic processes on its inlet surface.

#### 3.2. Solution of the problem

It is seen that in order to solve the diffusion problem, the change of the dissolved gas with time,  $C(0, t)$ , should

be determined, i.e., it is necessary first to solve the system of Eqs. (1)–(3), and then Eq. (4). Eqs. (1)–(4) can be solved only numerically. In order to make the problem mathematically tractable, some simplifying assumptions are made which are justified by the experimental evidence as it will be seen in Section 4.

It is assumed that

(1) The adsorption and dissociation processes are very fast and therefore their contribution to the delay time  $\tau$  is negligible [31].

(2) The fraction of the sites occupied by the molecules and atoms on the membrane surface fulfil the conditions  $\theta_a \ll 1$ ,  $\theta_m \ll 1$  [17,19,21,23].

(3) The rate of the gas transport into the membrane is much slower than the net rates of the solution and dissolution processes, i.e.,  $-k_{\text{dsol}}C(1 - \theta_a - \theta_m) + k_{\text{sol}}\theta_a \gg \gamma J_D$ .

These assumptions automatically lead to the following equations:

$$k_{\text{diss}}\theta_m = k_{\text{rec}}\theta_a^2, \quad (5)$$

$$k_{\text{ads}}p(1 - \theta_a - \theta_m) = k_{\text{des}}\theta_m, \quad (6)$$

and reduce Eqs. (1)–(3) to two linear differential equations:

$$\frac{d\theta_a}{dt} = k_{\text{dsol}}C - k_{\text{sol}}\theta_a, \quad (7)$$

$$\frac{dC}{dt} = -k_{\text{dsol}}C + k_{\text{sol}}\theta_a, \quad (8)$$

with boundary conditions for  $C(0, t)$ :  $t = 0$ :  $C(0, t) = C(0, 0)$  and  $t \rightarrow \infty$ :  $C(0, t) = C(0, \infty)$

It is physically reasonable to assume that  $C(0, 0) = 0$  at  $t = 0$ . Unfortunately this condition is rarely fulfilled in our experiment, since the first quantities of the permeated gas flux are registered at times, at which  $C(0, 0)$  is already different from zero. Therefore, in order to make our experimental data tractable within the frame of the present theoretical approach, it is assumed that  $C(0, 0) = \text{const.} \neq 0$  at  $t = 0$ .

A detailed description of the procedure for the solution of the Eqs. (7) and (8) is given for example in [32]. Following this procedure and taking into account that the right hand sides of Eqs. (7) and (8) are linearly dependent, for  $C(0, t)$

$$\begin{aligned} C(0, t) &= C_1 + C_2 \exp[-(k_{\text{dsol}} + k_{\text{sol}})t] \\ &= C_1 + C_2 \exp[-kt] \end{aligned}$$

is obtained [32]. Here  $C_1$  and  $C_2$  are integration constants and  $k$  is a kinetic coefficient accounting for the net result

of the kinetic dissolution and solution coefficients. Taking into account the above listed boundary conditions,

$$\begin{aligned} C(0, t) &= C(0, \infty) \left[ 1 - \left[ 1 - \frac{C(0, 0)}{C(0, \infty)} \right] \exp(-kt) \right] \\ &= C(0, \infty) [1 - A \exp(-kt)]. \end{aligned} \quad (9)$$

is finally obtained. Here  $A = [1 - (C(0, 0)/C(0, \infty))]$ .

The solution of Eq. (4) for a time dependent boundary condition on the membrane surface is given by the following Fourier series [25]:

$$\begin{aligned} C(x, t) &= \frac{2}{l} \sum_{n=1}^{\infty} \left( \frac{n\pi D}{l} \right) \left\{ \exp\left(-\frac{n^2\pi^2 Dt}{l^2}\right) \right. \\ &\quad \left. \int_0^t \exp\left(\frac{n^2\pi^2 D\tau}{l^2}\right) C(0, \tau) d\tau \right\} \sin\left(\frac{n\pi x}{l}\right). \end{aligned}$$

Substituting  $C(0, \tau)$  in the above equation with its equal — Eq. (9), the following is obtained:

$$\begin{aligned} C(x, t) &= \frac{2C(0, \infty)}{l} \sum_{n=1}^{\infty} \left( \frac{n\pi D}{l} \right) \left\{ \exp\left(-\frac{n^2\pi^2 Dt}{l^2}\right) \right. \\ &\quad \left. \int_0^t \exp\left(\frac{n^2\pi^2 D\tau}{l^2}\right) [1 - A \exp(-k\tau)] d\tau \right\} \\ &\quad \sin\left(\frac{n\pi x}{l}\right). \end{aligned} \quad (10)$$

Performing the integration in Eq. (10) and taking into account that

$$\begin{aligned} \sum_{n=1}^{\infty} \frac{\sin((n\pi x)/l)}{n} &= \frac{\pi(l-x)}{l} \quad \text{and} \\ \sum_{n=1}^{\infty} \frac{n \sin((n\pi x)/l)}{n^2 - (kl^2)/(D\pi^2)} &= \frac{\pi \sin[(k/D)^{1/2}(l-x)]}{2 \sin[(k/D)^{1/2}l]} \end{aligned}$$

[29],

$$\begin{aligned} C(x, t) &= \frac{2C(0, \infty)}{\pi} \left\{ \frac{\pi(l-x)}{2l} - A \exp(-kt) \right. \\ &\quad \times \frac{\pi \sin[(k/D)^{1/2}(l-x)]}{2 \sin[(k/D)^{1/2}l]} \\ &\quad \left. + \sum_{n=1}^{\infty} n \left[ \frac{A}{n^2 - (kl^2)/(D\pi^2)} - \frac{1}{n^2} \right] \right. \\ &\quad \left. \exp\left(-\frac{n^2\pi^2 Dt}{l^2}\right) \sin\left(\frac{n\pi x}{l}\right) \right\} \end{aligned} \quad (11)$$

is finally obtained.

As was explained in Section 2, the gas flux permeated  $J(t) = -(\partial C(x, t)/\partial x)|_{x=l}$  [2,25] through the membrane was measured in our experiment instead of  $C(x, t)$ . Substituting the obtained solution for  $C(x, t)$  into  $J(t)$  for the needed dependence,

$$J(t) = -D \frac{\partial C(x, t)}{\partial x} \Big|_{x=l} = \frac{C(0, \infty)D}{l} \left\{ 1 - \frac{Al \exp(-kt)}{\sin[(k/D)^{1/2}l]} \left(\frac{k}{D}\right)^{1/2} + 2 \sum_{n=1}^{\infty} (-1)^n \left[ \frac{An^2}{n^2 - (kl^2)/(D\pi^2)} - 1 \right] \exp\left(-\frac{n^2\pi^2Dt}{l^2}\right) \right\} \quad (12)$$

is obtained. In some cases, it is more convenient to treat the experimental data with the permeated gas quantity  $Q(t)$  instead of  $J(t)$ . Substituting  $J(t)$  from Eq. (12) into  $Q = S \int_0^t J(t) dt$  [2] and performing the integration,

$$Q(t) = S \int_0^t J(t) dt = J(\infty)S \left\{ t + \frac{Al(\exp(-kt) - 1)}{\sin[(k/D)^{1/2}l]} \left(\frac{1}{kD}\right)^{1/2} + 2 \sum_{n=1}^{\infty} \frac{(-1)^n l^2}{n^2 \pi^2 D} \left[ \frac{An^2}{n^2 - (kl^2)/(D\pi^2)} - 1 \right] \times \left[ \exp\left(-\frac{n^2\pi^2Dt}{l^2}\right) - 1 \right] \right\} \quad (13)$$

is obtained. Here  $J(\infty) = (DC(0, \infty))/l$  is the value of the gas flux at  $t \rightarrow \infty$ . At  $t \rightarrow \infty$ , (this is practically the time at which  $J(t) \rightarrow J(\infty) = \text{const.}$ ) all time dependent members in Eq. (13) tend to zero. Taking into account that

$$\sum_{n=1}^{\infty} \frac{(-1)^n}{n^2 - (kl^2)/(D\pi^2)} = \frac{\pi^2 D}{2kl^2} - \frac{\pi^2}{2l \sin[(k/D)^{1/2}l]} \left(\frac{D}{k}\right)^{1/2}$$

and

$$\sum_{n=1}^{\infty} \frac{(-1)^n}{n^2} = -\frac{\pi^2}{12}$$

[29],

$$Q(t) = J(\infty)S \left\{ t - \left[ \frac{l^2}{6D} + \frac{A}{k} \right] \right\} = J(\infty)S \{ t - \tau \} \quad (14)$$

is obtained for the permeated gas quantity at  $t \rightarrow \infty$ . Here,  $\tau$  denotes the total delay time of the permeation process.

Three possible cases exist:  $l^2/(6D) \cong A/k$ ,  $l^2/(6D) \gg A/k$  and  $l^2/6D \ll A/k$ .

The first expression describes the case when the rates of the surface reactions and the diffusion are comparable with each other and, therefore, with equal contribution to  $\tau$ , i.e., here the determined total delay time  $\tau$  is a sum of the delay times of the processes of diffusion  $\tau_D$  and the kinetic processes taking place on the membrane surface  $\tau_{kin}$ :  
 $\tau = \tau_D + \tau_{kin}$ .

The second expression describes the case when the surface processes are very fast and the observed delay time is determined mainly by the gas diffusion through the specimen. Taking into account that in this case the first member,  $\tau_D$ , accounting for the delay time due to the diffusion, is much larger than the second one,  $\tau_D \gg \tau_{kin}$  Eq. (14) reduces to the classical result,  $Q(t) = J(\infty)S \{ t - (l^2/(6D)) \}$ , quoted in Section 1. For this case the dependence  $J(\tau_D) = 0.6299J(\infty)$  [2,3] is also fulfilled. The fulfillment of this dependence shows that the permeation process is controlled mainly by the diffusion and, therefore, in the analysis of the experimental data it may be used as a criterion, whether the permeation process is purely diffusion controlled or not. For example in Fig. 1 this condition is not fulfilled and, therefore, the experimental results should be treated with Eq. (12).

The third expression,  $l^2/(6D) \ll A/k$ , describes the case when the diffusion process is much faster than the surface kinetic processes,  $\tau_D \ll \tau_{kin}$ . In this case, Eq. (14) reduces to  $Q(t) = J(\infty)S \{ t - (A/k) \}$  and the experimentally measured delay time  $\tau$  is mainly due to the processes which take place on the surface of the specimen. Substituting  $t$  with  $\tau_{kin} = A/k$  into Eq. (12) and taking into account that  $(l^2 k)/D \ll 1$  and that  $(\sin[(k/D)^{1/2}l]/l(k/D)^{1/2})|_{(kl^2)/D \rightarrow 0} \rightarrow 1$  for  $J(\tau_{kin})$ ,

$$b = 1 - \frac{J(\tau_{kin})}{J(\infty)} = A \exp(-A) \quad (15)$$

is obtained. The solution of this equation with respect to  $A$  is given by the omega function  $W$  [30]:

$$A = -W(-b).$$

It should be noted that only these values of  $b$  are physically meaningful which obey the inequality  $0 < b < 0.367894$  [30]. Therefore, as in the previous case this can be used for a preliminary assessment of the experimental data in order to decide, whether the permeation process is surface-reaction controlled or not. Taking into account that  $A = -W(-b)$  and that  $\tau_{kin} = A/k$  for the kinetic rate constant  $k$ , in this case

$$k = -\frac{W[-(1 - (J(\tau_{kin})/J(\infty)))]}{\tau_{kin}} \quad (16)$$

is obtained. The considerations used provide the answer of the question, formulated implicitly in Section 1, namely

how thick should be the membrane that the influence of the surface processes on the permeation measurements can be neglected. As it is seen from the analysis carried above, the condition for diffusion controlled permeation is  $\tau_D \gg \tau_{kin}$ . Solving this inequality with respect to  $l$ ,  $l^2 \gg (6DA)/k$  is obtained.

Concluding this section it should be noted that the treatment of the experimental permeation data, using only the equations cited in Section 1, should be done in the case when  $J(\tau_D) = 0.6299J(\infty)$ , i.e., in the case when the inequality  $l^2/(6D) \gg A/k$  is fulfilled. In some cases these conditions are not fulfilled and therefore it is recommended, to treat the experimental data with Eq. (12) in order to avoid erroneous conclusions.

#### 4. Experimental results and discussion

The analysis developed assumes that the observed discrepancy between the theory and experiment is due to surface reactions on the inlet surfaces of the specimens. To check the validity of this assumption and gain proof in its support specimens prepared from STE890 steel (C – 0.18, Si – 0.23, Mn – 1.4, P – 0.007, S – 0.003, Cr – 0.025, Mo – 0.496 in wt%) and the amorphous  $Fe_{40}Ni_{40}Mo_4B_{16}$  alloy have been studied. The specimens from STE890 steel were prepared from steel sheets first submitted to plastic deformation and then annealed at 1150°C for 3 h. After annealing the samples were cooled down in the furnace. The samples from the amorphous  $Fe_{40}Ni_{40}Mo_4B_{16}$  alloy were made from as-quenched amorphous ribbons without any preliminary mechanical or thermal treatments. Three types of samples have been prepared from these specimens: as-obtained and covered with thin coating from Pd or amorphous carbon. The processes discussed here take place on the membrane surface. Hence it should be expected that a possible change of the surface conditions will lead to changes in the observed functional dependencies of the hydrogen transport through the studied samples. Provided that Eq. (12) is valid, the coating with Pd or with amorphous carbon respectively, will change only the surface characteristics of the sample but not the hydrogen permeation or diffusivity.

A typical experimental curve obtained is shown in Fig. 1. The best fits by non-linear regression using both Eq. (12) and the classical solution of the Fick equation [2] are also shown in Fig. 1. It is seen that the hydrogen flux calculated from Eq. (12) is very close to the experimentally obtained one. On the contrary the flux calculated from the classical equations [2] deviates considerably. This result is an indirect proof that the observed discrepancy between the experiment and the classical theory is a result of surface processes.

All experimental curves  $J = J(t)$  obtained from different samples, temperatures and hydrogen pressures were analyzed by non-linear regression using Eq. (12). The

values of the hydrogen steady state flux,  $J(\infty)$ , the diffusion coefficient,  $D$ , the kinetic rate constant,  $k$ , and the parameter,  $A$ , were derived.

At steady state  $d\theta_m/dt = 0$ ,  $d\theta_a/dt = 0$  and  $dC/dt = 0$ , and the system of Eqs. (5)–(8), reduces to

$$k_{diss}\theta_m = k_{rec}\theta_a^2, \quad (17)$$

$$k_{ads}p = k_{des}\theta_m, \quad (18)$$

$$k_{dso}C = k_{sol}\theta_a. \quad (19)$$

It should be noted that in this case Eqs. (7) and (8) are linearly dependent and thus reduce to Eq. (19). The solution of the above system with respect to  $\theta_a$ ,  $\theta_m$  and  $C(0, \infty)$  leads to an expression similar to Sievert's rule [28]:

$$C(0, \infty) = \frac{k_{dso}}{k_{sol}} \sqrt{\frac{k_{ads}k_{dis}}{k_{des}k_{rec}}} \sqrt{p} = \frac{1}{k_s} \sqrt{\frac{k_a}{k_d}} \sqrt{p} \\ = K(T)\sqrt{p}. \quad (20)$$

Here  $k_a = k_{ads}/k_{des}$ ,  $k_d = k_{rec}/k_{diss}$ ,  $k_s = k_{sol}/k_{dso}$  [23] and  $K(T)$  is a gas solubility coefficient. Substituting Eq. (20) into  $J(\infty) = (DC(0, \infty))/l$  yields  $J(\infty) = ((DK)/l)\sqrt{p} = (P/l)\sqrt{p}$  — Richardson's Law of Permeation [21]. The product  $P = DK$  is commonly defined as gas permeation. Therefore,  $J(\infty)$  at constant temperature should be linearly dependent on the square root of the pressure in the inlet chamber  $\sqrt{p}$  and the slopes should determine the hydrogen permeation,  $P$ , through the specimen.

The values of the steady state hydrogen flux  $J(\infty)$  for the as-prepared STE890 plotted vs.  $\sqrt{p}$  are shown in Fig. 3. It is seen that the law  $J(\infty) \sim \sqrt{p}$ , is obeyed at nearly all experimental pressures,  $p$ , with the exception of the low pressures, where the  $J(\infty)$  curve deviate from the square root law. This deviation is probably due to the assumptions made in Section 3 —  $\theta_a \ll 1$  and  $\theta_m \ll 1$ , which may not be correct at low  $T$  and  $p$ . In this case Eq.

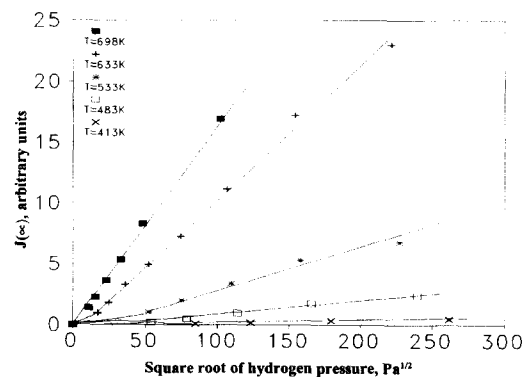


Fig. 3. Steady state hydrogen fluxes  $J(\infty)$  in the 413–698 K temperature range through as prepared specimen of STE890 steel as a function of the square root of the pressure  $p$  in the inlet chamber.

(20) obtained by the Eqs. (17)–(19) is not correct and  $J(\infty) = J(\infty, p)$  dependence should be determined from Eqs. (1)–(3) at  $d\theta_m/dt = 0$ ,  $d\theta_a/dt = 0$ ,  $dC/dt = 0$  and

$$-k_{\text{dsol}}C(1 - \theta_a - \theta_m) + k_{\text{sol}}\theta_a \gg \gamma J_D:$$

$$k_{\text{ads}}p(1 - \theta_a - \theta_m) - k_{\text{des}}\theta_m - k_{\text{diss}}\theta_m + k_{\text{rec}}\theta_a^2 = 0, \tag{21}$$

$$k_{\text{dsol}} \frac{J(\infty)l}{D} (1 - \theta_a - \theta_m) - k_{\text{sol}}\theta_a + k_{\text{diss}}\theta_m - k_{\text{rec}}\theta_a^2 = 0, \tag{22}$$

$$-k_{\text{dsol}} \frac{J(\infty)l}{D} (1 - \theta_a - \theta_m) + k_{\text{sol}}\theta_a = 0. \tag{23}$$

In Eqs. (22) and (23)  $C(0, \infty)$  is substituted with its equal  $C(0, \infty) = (J(\infty)l)/D$ . By solving this system with respect to  $\theta_a$ ,  $\theta_m$  and  $J(\infty)$ ,

$$\left(\frac{l}{D}\right)^2 J^2(\infty) - \frac{k_s k_a}{k_d} \frac{l}{D} p J(\infty) - \frac{k_s^2 k_a}{k_d} p (k_a p + 1) = 0 \tag{24}$$

is obtained. The same dependence of  $J(\infty)$  on the pressure  $p$  as the one observed in Fig. 3 is obtained from the solution of Eq. (24) with respect to  $\sqrt{p}$ .

The analysis of Eqs. (20) and (24) show that the transition from  $J(\infty) \sim \sqrt{p}$  to  $J(\infty) \sim p$  is due to the influence of the adsorption and dissociation processes, since they are responsible for the dynamics of  $\theta_a$  and  $\theta_m$  sites. This result differs from the explanation accepted in the literature [17–24], where it is assumed that the observed functional dependence  $J(\infty, p)$  is due to the transition from diffusion to surface reaction controlled permeation. If the above stated result is correct, it should be expected that coating with materials (such as Pd or amorphous carbon) which accelerate the adsorption and dissociation will lead to fulfillment of the square root law and

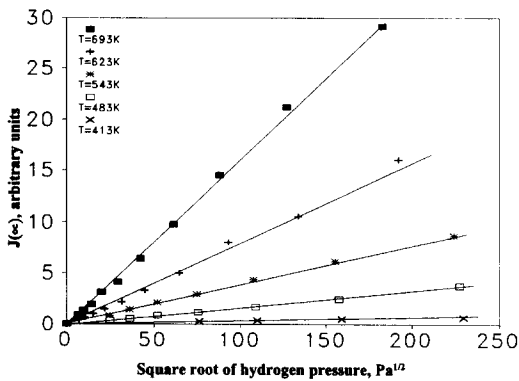


Fig. 4. Steady state hydrogen fluxes  $J(\infty)$ , through the same specimen of STE890 steel and for the same temperature range, as in Fig. 3, covered with a thin Pd layer, as a function of the square root of the pressure  $p$  in the inlet chamber.

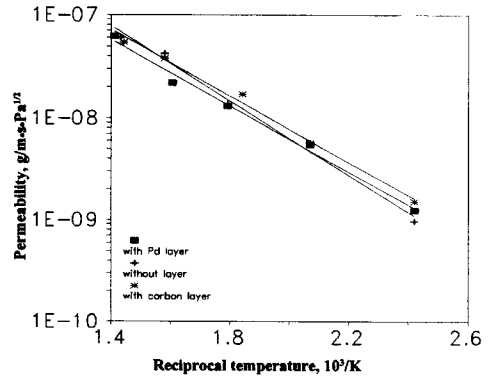


Fig. 5. Arrhenius plot of the hydrogen permeability  $P$ , for the STE890 steel. J – as prepared, A – covered with Pd and K – covered with amorphous carbon.

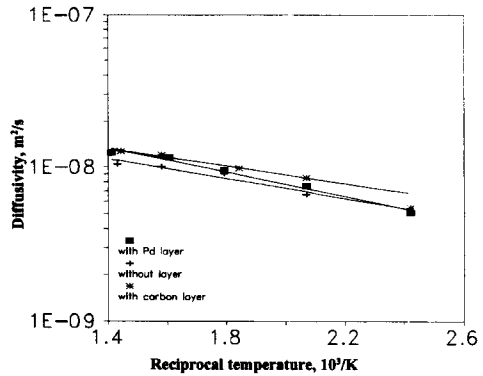


Fig. 6. Arrhenius plot of the hydrogen diffusivity  $D$ , for the STE890 steel. J – as prepared, A – covered with Pd and K – covered with amorphous carbon.

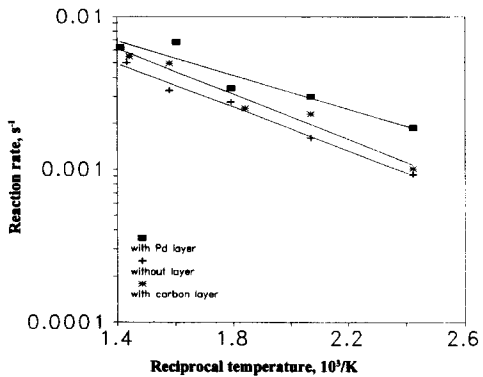


Fig. 7. Arrhenius plot of the adsorption rate constant  $k$ , for the STE890 steel. J – as prepared, A – covered with Pd and K – covered with amorphous carbon.

Table 1

Values of the hydrogen permeability  $P_0$ , the hydrogen diffusivity coefficient  $D_0$ , and the kinetic coefficient of the adsorption reaction  $k_0$  and their activation energies  $E_p$ ,  $E_D$ , and  $E_k$  for STE890 steel and the amorphous  $\text{Fe}_{40}\text{Ni}_{40}\text{Mo}_4\text{B}_{16}$  alloy obtained from the Arrhenius plots in Figs. 5–8

Specimen	Diffusion		Permeability		Kinetic rate constant	
	$D_0$ ( $\text{m}^2/\text{s}$ )	$E_D$ (kJ/mol)	$P_0$ ( $\text{g}/(\text{m s Pa}^{0.5})$ )	$E_p$ (kJ/mol)	$k_0$ ( $\text{s}^{-1}$ )	$E_k$ (kJ/mol)
STE890 (J)	$3.2 \times 10^{-8}$	6.12	$2.8 \times 10^{-5}$	34.92	$4.9 \times 10^{-2}$	13.7
STE890 (A)	$4.7 \times 10^{-8}$	7.53	$1.07 \times 10^{-5}$	31.00	$4.2 \times 10^{-2}$	10.73
STE890 (K)	$3.3 \times 10^{-8}$	5.45	$1.36 \times 10^{-5}$	31.06	$6.7 \times 10^{-2}$	14.2
$\text{Fe}_{40}\text{Ni}_{40}\text{Mo}_4\text{B}_{16}$	$2.5 \times 10^{-9}$	29.6	–	–	–	–

validity of Eq. (12) for all temperatures and pressures applied [11].

The steady state hydrogen fluxes at different temperatures, measured for specimens covered with Pd, are plotted vs. square root of the pressure in Fig. 4. It is seen that the  $J(\infty) \sim \sqrt{p}$  law is obeyed for all pressures and temperatures studied. Similar results as in Fig. 4 are observed for the specimens covered with amorphous carbon. Therefore, for the particular case of hydrogen permeation studied here it can be concluded that the transition from  $J(\infty) \sim \sqrt{p}$  to  $J(\infty) \sim p$  at low pressure is due to limitations imposed on the hydrogen permeation from adsorption and dissociation. Hydrogen permeation experiments carried out at low temperatures and pressures should be performed on specimens, covered with a thin layer of a material which accelerates adsorption and dissociation in order to make Eq. (12) applicable.

Figs. 5–7 present Arrhenius plots of hydrogen permeation,  $P$ , (Fig. 5), diffusion coefficient,  $D$ , (Fig. 6) and kinetic coefficient,  $k$ , (Fig. 7) derived from Eq. (12) for as-prepared and coated with Pd or amorphous carbon specimens. It is seen that the Arrhenius plots of  $P$  and  $D$  overlap for all specimens in the whole temperature range

studied. On the contrary, in Fig. 7 it can be seen that the kinetic coefficient,  $k$ , is strongly affected from the coating material, which accounts for the assumption of surface processes involvement in the hydrogen permeation kinetics.

The theory developed has been tested also on experimental data for amorphous  $\text{Fe}_{40}\text{Ni}_{40}\text{Mo}_4\text{B}_{16}$  alloy obtained in [4]. Fig. 8 shows the Arrhenius plot of diffusion coefficients  $D$  obtained for this data using Eq. (12) (solid squares). These values for  $D$  are compared with the data of Lin and Perng [5] for the amorphous  $\text{Fe}_{40}\text{Ni}_{38}\text{Mo}_4\text{B}_{18}$  alloy obtained by electrochemical permeation (open squares). A good agreement can be observed despite the different methods applied.

The values for  $P_0$ ,  $D_0$ ,  $k_0$ ,  $E_p$ ,  $E_D$ , and  $E_k$ , for STE890 steel, and the amorphous  $\text{Fe}_{40}\text{Ni}_{40}\text{Mo}_4\text{B}_{16}$  alloy, derived from Arrhenius plots in Figs. 5–8, are presented in Table 1.

## 5. Conclusions

A method for the determination of the hydrogen diffusion coefficient  $D$  through thin membranes has been developed taking into account the kinetic processes on the membrane surface. The theoretical and experimental approach developed for the determination of the hydrogen diffusivity and hydrogen permeation provides the possibility to obtain reliable results and can be applied to study the permeation of hydrogen into different materials. It is shown that the rate of hydrogen permeation is influenced by processes on the specimen's surface. This is particularly true when the hydrogen permeation into amorphous ribbons is studied. A criterion was set out for the determination when the surface kinetic processes should be taken into account. The results obtained show that the method proposed leads to reliable results, comparable to those of other authors [5,31].

## Acknowledgements

The authors are grateful to the Bulgarian National Scientific Research Foundation contracts TN-482/94 and

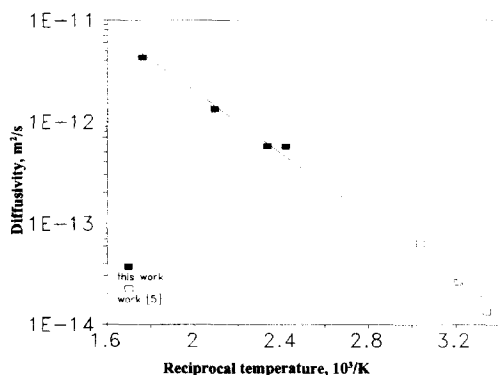


Fig. 8. Arrhenius plot of the diffusion coefficient  $D$ , for the amorphous  $\text{Fe}_{40}\text{Ni}_{40}\text{Mo}_4\text{B}_{16}$  alloy in the 428–568 K temperature range (solid squares), compared with the experimental data of Lin and Perng [5], obtained by the electrochemical permeation method, for the amorphous  $\text{Fe}_{40}\text{Ni}_{38}\text{Mo}_4\text{B}_{18}$  alloy in the temperature range – 303–348 K (open squares).



TN-323/93 for the financial support of the present research.

## References

- [1] H. Daynes, Proc. R. Soc. 97A (1920) 286.
- [2] Y. Adda, J. Philibert, La Diffusion dans les Solides, Vol. I (Presses Universitaires de France, 1966).
- [3] M.A.V. Devanathan, Tech. Report No. ONR/551/22/NR 036-028, 1961.
- [4] J. Georgiev, K. Russev, L. Stojanova, J. Mater. Sci. Tech. 2 (4) (1994) 29.
- [5] J.-J. Lin, T.-P. Perng, Acta Metall. Mater. 39 (1991) 1101.
- [6] J. Georgiev, Ch. Maltsev, L. Saraivanov, N. Stanev, I. Pechenjakov, in: Proc. 3rd Int. Conf. on High Nitrogen Steels HNS'93 part II, eds. V. Gavriljuk and V. Nadutov, Sept. 14–16, 1993, Kiev, Ukraine.
- [7] E. Fromm, E. Gebhardt, Gase und Kohlenstoff in Metallen (Springer, Berlin, 1976).
- [8] T. Tanabe, Y. Yamanishi, K. Sawada, S. Imoto, J. Nucl. Mater. 122&123 (1984) 1568.
- [9] A.J. Kumnick, H.H. Johnson, Metall. Trans. 6A (1975) 1087.
- [10] W.I. Telkov, L.A. Andreev, G.L. Malyutina, Russ. J. Phys. Chem. (USSR) 54 (1980) 2745, in Russian.
- [11] K. Nakamura, H. Uchida, E. Fromm, J. Less-Common Met. 80 (1981) P19.
- [12] A. Pospieszczyk, J.A. Tagle, J. Nucl. Mater. 105 (1982) 14.
- [13] H.H. Johnson, Scr. Metall. 23 (1989) 1265.
- [14] E. Wicke, F. Verfuss, A.S. Schmidt, Z. Metallkd. 74 (1983) 7.
- [15] J. Xu, X.K. Sun, W.X. Chen, Y.Y. Li, Acta Metall. Mater. 41 (1993) 1455.
- [16] M. Kano, N. Kagawa, S. Koike, K. Furuya, T. Suzuki, Acta Metall. 36 (1988) 1553.
- [17] Ali-Khan, K.J. Dietz, F. Waelbroeck, P. Wienhold, J. Nucl. Mater. 76&77 (1978) 337.
- [18] D.M. Grant, D.L. Cummings, D.A. Blackburn, J. Nucl. Mater. 152 (1978) 139.
- [19] E. Rota, F. Waelbroeck, P. Wienhold, J. Winter, J. Nucl. Mater. 111&112 (1982) 233.
- [20] M. Braun, B. Emmoth, F. Waelbroeck, P. Wienhold, J. Nucl. Mater. 93&94 (1980) 861.
- [21] M.A. Pick, K. Sonnenderg, J. Nucl. Mater. 131 (1985) 208.
- [22] R.A. Causey, M.I. Baskes, J. Nucl. Mater. 145–147 (1987) 284.
- [23] P.M. Richards, J. Nucl. Mater. 152 (1988) 246.
- [24] E. Serra, A. Perudjo, J. Nucl. Mater. 223 (1995) 157.
- [25] H.S. Carslaw, J.C. Jaeger, Conduction of Heat in Solids (Iarendon, Oxford, 1964)
- [26] S. Dushman, Scientific Foundations of Vacuum Technique (Inostrannaja Literatura, Moscow, 1950) (Russian version).
- [27] E.A. Moelwyn-Hughes, Physical Chemistry (Pergamon, London, 1961).
- [28] A.A. Zjuhovitski, L.A. Shwarzman, Physical Chemistry (Metallurgia, Moscow, 1976) (in Russian).
- [29] A.P. Prudnikov, Y.A. Bruichkov, O.I. Marichev, Integrals and Series, Vol. I (Nauka, Moscow, 1981) (in Russian).
- [30] F.N. Fritsch, R.E. Schafer, W.P. Crowley, Solution of the Transcendental Equation  $W \exp(W) = x$ , Commun. ACM 16 (2) (1973).
- [31] B.A. Kolachev, Y.W. Levinskij, eds., Handbook for Interaction of the Metals with Gases, Constants and Other Data (Metallurgia, Moscow, 1987) (in Russian).
- [32] E. Kamke, Differentialgleichungen, Lösungsmethoden und Lösungen, Vol. 6 (verb. Auflage, Leipzig, 1959).